Energetic analysis and optimization of a MACCEPA actuator in an ankle prosthesis

Geeroms, Joost; Flynn, Louis; Jimenez-Fabian, Rene; Vanderborght, Bram; Lefeber, Dirk

Published in:
Autonomous Robots

DOI:
10.1007/s10514-017-9641-1

Publication date:
2018

Autonomous Robots manuscript No.
(will be inserted by the editor)

Energetic analysis and optimization of a MACCEPA actuator in an ankle prosthesis.

Energetic evaluation of the CYBERLEGs alpha-prosthesis variable stiffness actuator during a realistic load cycle.

Joost Geeroms · Louis Flynn · Rene Jimenez-Fabian · Bram Vanderborght · Dirk Lefeber

Received: date / Accepted: date

Abstract The use of active prostheses for lower limb replacement brings new challenges like power optimization, energy efficiency and autonomy. The use of series and parallel elasticity is often explored to reduce the necessary motor power but this does not necessarily have a positive influence on the energy consumption of the prosthesis. This paper presents the experiments performed with the variable compliance actuator used in an active ankle prosthesis and the electromechanical model of this actuator. The results show that the measurements can be matched using the model, and this model can thus be used to optimize the energy efficiency of the actuator. Simulations show that the electrical efficiency can be increased by 10% compared to parameters selected by an optimization method that only takes mechanical properties into account.

Keywords Actuator · Energy efficiency · CYBERLEGs · Ankle · Prosthesis · human gait · series elasticity

1 Introduction

A large number of people worldwide undergo a lower limb amputation due to multiple possible causes: cardiovascular diseases, trauma, congenital causes and cancer being the most prevalent [1]. Combining the factors of an increasing average age worldwide and a higher risk of dysvascular amputation for elderly [2], shows the need for better performing lower limb prostheses. As a result, the research on prosthetic devices which are able to provide a natural gait pattern has become more important over the last decade. Trying to approximate a healthy human ankle behavior, there is a clear advantage of prostheses making use of active components over purely passive prostheses, as in a healthy gait cycle there is also a net positive energy balance [3]. It has been shown that providing an active push-off with correct timing at the ankle and can decrease the metabolic rate of walking for amputee subjects compared to walking with a passive prosthesis [4]. Several prototypes have been developed using series springs [5] and nonlinear [6] or variable [7] transmission systems for power optimization. Multiple prototypes have been investigated which use compliant actuation to successfully reduce the peak power and thus the weight of (lower limb) prosthetic devices when compared to a direct drive solution [8–10]. Zhu et al. [11] investigated the effect of having actuated and stiffness adjusted toe joints. One of the major disadvantages of most of these active prostheses is that their weight is still significantly higher than that of passive devices, mostly consisting of carbon fiber springs for passive ankles and dampers for passive knees. Apart from the motor and gearing, these powered prostheses not only require electronics such as motor drivers and a control unit, but also a power source such as a battery pack. For example, the weight of a BiOM (active) ankle prosthesis is about 2.3 kg electronics and batteries included, while a passive Ossur Flex-foot including cover only weighs 500 g. The prototype investigated in this work, which is not optimized for weight, weighs 1.5 kg, without electronics, batteries and cover.

Several research papers present simulations and optimizations of the output characteristics of actuators with series elasticity for different spring stiffnesses [12]. Most often these optimizations minimize the mechani-

J. Geeroms
Robotics Research Group, Vrije Universiteit Brussel,
Pleinlaan 2 1050 Brussels, Belgium
Tel.: +123-45-678910 E-mail: jgeeroms@vub.ac.be

cal energy or the mechanical power peak at the output of the actuator [13–16, 11]. Also when investigating the effects of parallel elasticities on the actuator, often only these mechanical properties are investigated [17–19]. These optimization techniques however do not necessarily lead to a lower electrical energy consumption as the effects of the motor efficiency and the torque- and velocity dependency of it are often neglected in this case. This can lead to a significant increase in losses, as a optimized mechanical output will comprise parameters which lead to minimized motor velocities and torques, which is exactly the region of the motor operation with the lowest efficiency [20, 21]. In some cases, the motor characteristics are taken into account for the design of a compliant actuator [22–25]. One of the important reasons for choosing series elasticity in an actuator is the possibility of power amplification as described by [10], where the authors simulate and show an amplification of the possible output power by a factor 1.4 over the power limit of the power source.

The actuator described in this paper is part of the CYBERLEGs project [26]. This project aims to restore the walking ability for people who underwent lower limb amputation due to dysvascular disease by replacing their lost limb with an active prosthesis and also supporting the rest of the body by means of an active hip-knee-ankle orthosis [27] and a high level cognitive control system, including a fall detection system [28]. As the aim is to ultimately have a wearable system, the energy consumption of all of the components needs to be reduced as much as possible.

In this paper we investigate in detail the energy consumption of a variable stiffness actuator for realistic load cycles at different velocities and with different precompression values for the series spring, causing the actuator to have a different stiffness characteristic. The efficiency of the motor driver, the motor, the gearbox and the output mechanics will be investigated for different load cycles and the system will be compared to a direct drive application. An electromechanical motor model is then developed and evaluated based on the measurements. This model can be used to define an optimal configuration for the actuator, which can be compared to the configuration based on an optimization method using only mechanical properties. The actuator used in this work is presented in Section 2. Section 3 shows the model and measurement setup and Section 4 the results of the measurements and simulations which are then discussed in section 5.

2 Actuator architecture

The actuator investigated in this paper has been implemented in the CYBERLEGs α-prosthesis. Figure 1 shows a walking experiment with the complete ankle-knee prosthesis.

The actuator is a MACCEPA: a variable compliance actuator which was used before in different bio-inspired robotic applications. The design used for this actuator is a variation on the concept as described in [29] using a cable transmission, but instead using rigid linkages presented in [30]. By eliminating the cable, all possible problems with tensioning, fastening and wearing of it were avoided. The proposed actuator configuration is shown in Figure 2. For this lay-out, we can calculate the torque around the ankle joint as a function of the motor angle, the moment arm lengths and the precompression force. Using the symbols of the schematic in figure 2, the length of link C as a function of the angle α can be determined using basic goniometric formulas:

$$C(\alpha) = B\cos\alpha + A\left[1 - \left(\frac{B}{A}\sin\alpha\right)^2\right]^{1/2} \tag{1}$$

The force perpendicular to link C other hand is a function of the angle α as well as the spring constant k and the precompression length P:

$$f(\alpha, P) = \frac{kB(P + A + B - C(\alpha))\sin\alpha}{A\left[1 - \left(\frac{B}{A}\sin\alpha\right)^2\right]^{1/2}} \tag{2}$$

These equations can be combined to get the torque around the ankle joint:

$$T(\alpha) = C(\alpha)f(\alpha, P) \tag{3}$$

The method of selecting the characteristics and components for the ankle actuator is described in [30] and [31]. A 200 Watt Maxon EC-4pole motor was selected for the actuator. Fitted with a gearbox with a ratio of 86:1 and another helical gear with ratio 10:1, this motor is able to provide the desired torque pattern. For the series spring, a die spring with a spring constant of 132 N/mm was chosen. Figure 3 shows the ankle prosthesis. The motor in this prototype is situated next to the tube above the ankle joint, which connects to the knee prosthesis. The ankle joint itself is not meant to be connected to an amputee socket as it was designed to be part of an integrated ankle-knee prosthesis.

From the ankle kinematics during level ground walking the target torque and angle can be calculated that have to be achieved at the prosthetic ankle joint. With the equations we have of the MACCEPA actuator, we

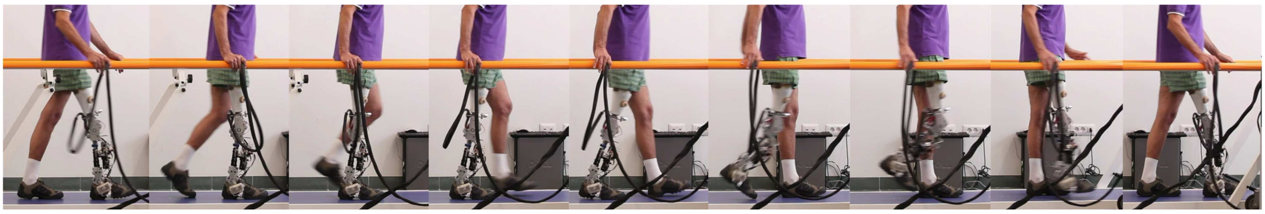

Fig. 1 Timelapse of a walking experiment: a transfemoral amputee walking with the CYBERLEGs α-prosthesis on a catwalk. This experiment was approved by the Ethical Committee of the Don Gnocchi Foundation.

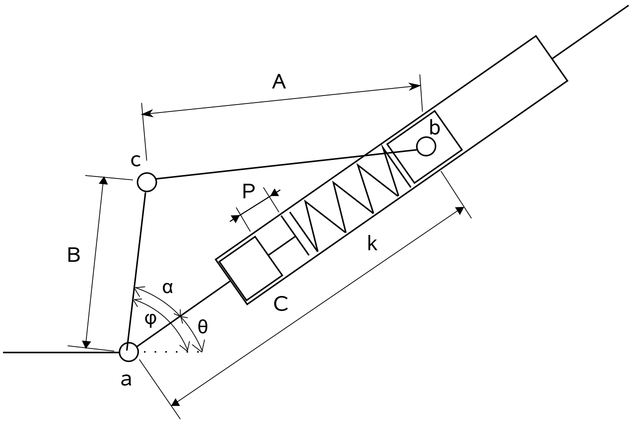

Fig. 2 Configuration of the sliding-bar MACCEPA. Point a represents the ankle joint, the linkage which is connecting a and b represents the foot and the linkage between points a and c is the moment arm which is driven by the ankle motor. α is the angle between the moment arm and the ankle, θ is the ankle angle, between the lower leg and the foot, and φ is the sum of both, which is the angle between the lower leg and the moment arm, being the motor lever arm.

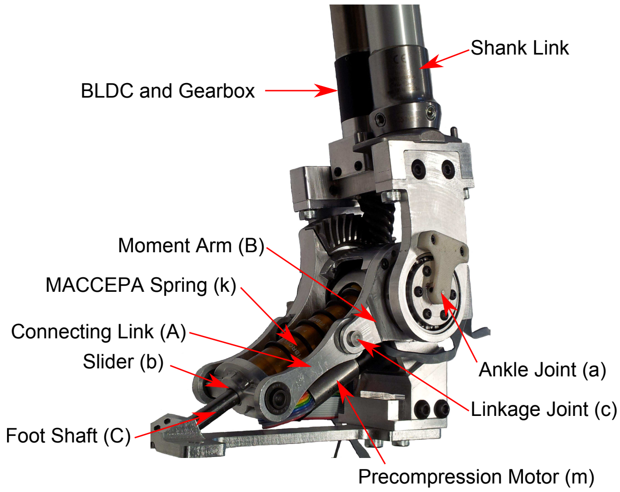

Fig. 3 The CYBERLEGs alpha-prosthesis ankle joint which has been tested in this paper. The picture shows the motor above the ankle joint, connecting to the moment arm which is situated in the foot. The motor changes the moment arm angle, compressing the spring and causing a torque around the ankle joint. A small, high geared motor changes the precompression of the spring without changing the equilibrium position.

can calculate the desired motor output position throughout the gait cycle so that the actuator provides this target. After doing that, different optimization methods can be used to select the optimal spring stiffness and precompression for the actuator. In the case of this actuator, the peak mechanical power that has to be provided by the actuator was minimized, and the minimization technique used in [31] shows an optimum at a precompression of 7mm for a spring with a stiffness of 130 N/mm when the actuator is simulated to match the target trajectory perfectly. The reasoning for this optimization method is that by reducing the peak power that needs to be provided the size of the motor can be minimized. Using this method however does not take into account the overall electrical energy consumption of the prosthesis as no model of the motor is included in the analysis, so only the mechanical energy is taken into account.

3 Materials and Methods

Using the components selected in [31], an electromechanical model of the actuator was created in Simulink to predict the energy consumption of the actuator during a loading cycle which is representative for one human step, which can then be verified using the experiments. The equations used for the model, including both the electrical and mechanical properties of the actuator are:

$$\begin{aligned} L\frac{d(i)}{dt} + Ri + \frac{k_(\omega)}{n_{total}}\dot{\varphi} &= V \\ J\ddot{\varphi} + b\dot{\varphi} + n_{total}T_{maccepa} &= k_m i \end{aligned} \tag{4}$$

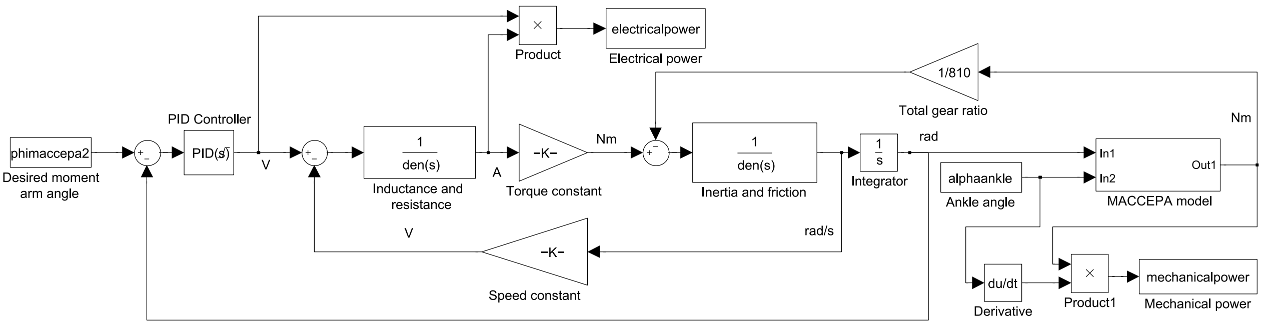

Fig. 4 Overview of the Simulink model. The moment arm angular position and angular position of the joint are used as inputs, the mechanical and electrical power can be calculated from the model.

With:

$$
\begin{aligned}
L &= \text{Terminal inductance (H)} \\
R &= \text{Terminal resistance } (\Omega) \\
k_(\omega) &= \text{Speed constant (Vs/rad)} \\
n_{total} &= \text{Total reduction ratio} \\
&\quad \text{(gearbox } + \text{ helical gear)} \\
J &= \text{Moment of inertia (kgm}^2\text{)} \\
b &= \text{Friction coefficient (Nm} * \text{s/rad)} \\
k_m &= \text{Torque constant (Nm/A)} \\
i &= \text{Motor current (A)} \\
V &= \text{Motor voltage (V)} \\
T_{maccepa} &= \text{Actuator output torque (Nm)} \\
\varphi &= \text{Moment arm angular position (rad)}
\end{aligned}
\tag{5}
$$

All of the motor parameters can be found in the datasheet. A profile for the actuator to follow is needed to calculate the energy efficiency over. This provides the desired moment arm position φ and the desired angular position of the output joint, which is needed to calculate $T_{maccepa}$. To measure the energy efficiency of the actuator any trajectory could be applied, but in order to get a realistic estimation of the energy consumption during normal walking the choice was made to apply the same trajectory as the prosthesis would typically follow if it would be used by the ideal amputee, one who walks with the same kinematics of an average healthy individual. For this reason, the trajectories used for the trials are the biomechanical joint torque and angle data of a healthy human's ankle [32]. These data give an average value of the ankle joint angle and torque, normalized for body weight and for one stride. This dataset provides both a desired angular trajectory and a torque trajectory. Using Equation (3) and the described torque trajectory, the necessary moment arm angle is calculated for different precompression values, ranging from 0 to 18mm. This is done by subtracting the torque calculation from the biomechanical torques and minimizing the result using the MATLAB fminbnd function. This results in several sets of moment arm positions which are used as inputs for the simulation. The angular position of the ankle is used to calculate the torque using φ and Equation (3). The simulation is used to mimick the different walking velocities tested during the experiments. Figure 4 shows the Simulink model with the described inputs. Both the mechanical and electrical power can be calculated using the model.

The parameters found in the datasheet will have to be adapted to the experimental set-up. For example, as the resistance of the motor windings is small, an estimation of the resistance of the cables and connectors used in the setup will have to be added. The inertia of the actuator itself is added as well as an estimate of the friction coefficient in the gearbox and rest of the actuator. This overall friction is a difficult parameter to estimate beforehand as it depends on a lot of variables like machining quality, surface finish, lubrication and assembly of parts and bearings.

It is possible to test the energy consumption of the prosthesis during walking experiments. However, for the amputee to walk with the prosthesis using a gait cycle which is repeatable and can be used for comparison to the simulations requires a large amount of training and effort of the amputee. For this reason a test setup was developed which can be used to apply any desired output angle trajectory to the prosthetic ankle. The ankle actuator itself can follow any torque trajectory within the actuator bandwidth limitations at the same time. The setup consists of a firm metal cage to which the actuator is attached. Parallel to the joint, a torque sensor is placed to be able to accurately measure the joint torque without using the mechanical model of the MACCEPA, defined by Equation (3). The other side of the torque sensor is connected to a DC motor with high gearing, which will be referred to as the output motor. This test setup makes it possible to apply any desired output kinematics to an actuator and test its behavior.

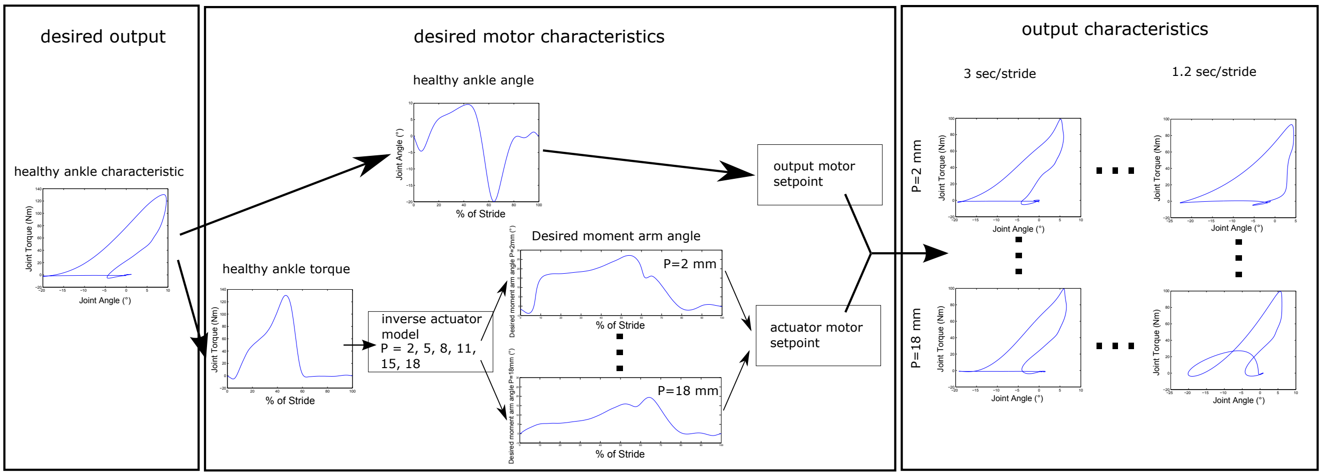

Fig. 5 Overview of the experimental setup: starting from the biomechanical ankle characteristic the desired motor characteristics for different precompressions P are calculated using the motor model, leading to different output characteristics at different walking velocities.

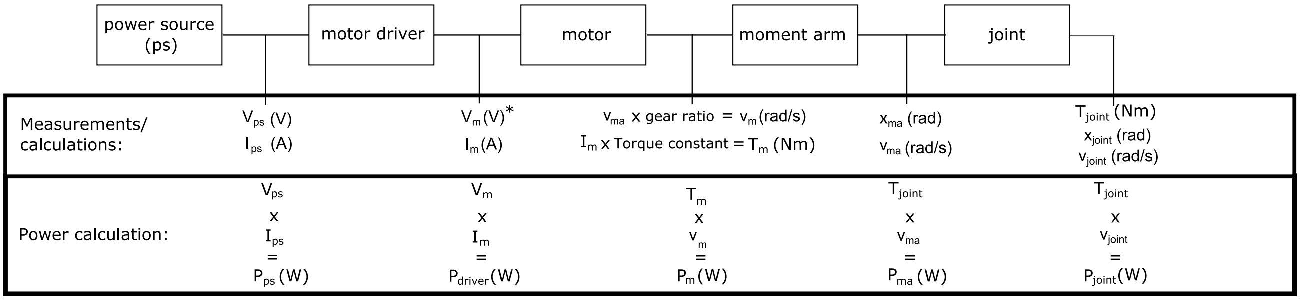

Fig. 6 Overview of the power measurements in the test setup. The power is calculated at five different locations inside the actuator from the power supply to the output. *The calculation for V_m can be found in Equation 6.

The principle of the experiment and calculation of the setpoints of the motors is clarified in Figure 5. The principle is the same as described for the actuator simulations, yet the ankle angle trajectory is used as setpoint for the output motor and the moment arm angle trajectory as setpoint for the actuator motor.

Both motors are driven by MAXON EPOS2 70/10 drivers and these are controlled by a NI sbRIO 9623. During the experiment the joint angle, moment arm angle and the torque around the ankle are recorded, as well as the power supply voltage, the current to the actuator driver and the motor current of the actuator motor. The current to the driver is measured using a Honeywell CSNE151 sensor, the motor current is outputted by the EPOS2 driver and the angles are measured by absolute magnetic encoders (AS5048A). From these variables the power can be calculated at different positions of the actuation, as can be seen in Figure 6, which shows the different variables that are measured and calculated from the measurements. The motor voltage is calculated using Equation (6):

$$V_m = k(\omega)v_m + Ri_m + L\frac{d(i_m)}{dt} \tag{6}$$

The power is measured between the power source and the motor driver (source power), between the driver and the motor (driver power), at the output of the motor (motor power), at the actuator moment arm (moment arm power) and at the joint (joint power). It is worth noting that the source and driver power is electrical power, while the motor, moment arm and joint power are mechanical power.

By taking the ratio of these powers the efficiencies of the different steps are calculated. By doing this for different walking velocities and spring precompression values, the effect of these on the efficiencies of the different components and the overall efficiency of the actuator is evaluated.

In these experiments, the precompression of the spring is changed in between the different experiments and the energetic consumption of the precompression motor is not taken into account. This precompression motor is a low-power (8W) and low-velocity motor, meaning the precompression can only be changed over several steps and the motor is not used to add energy to the walking cycle.

4 Results

In total, 6 different precompression values were investigated: 2, 5, 8, 11, 15 and 18 mm, which represent the whole possible range of precompressions for the actuator. All of these were tested at different walking velocities, being 1.2, 1.3, 1.5, 2, 2.5 and 3 seconds per stride. The results are first introduced and after this organized as follows: - Introduction and data representation
- Measurements energy losses
- Comparison to modeling results
- Optimization of the efficiency

4.1 Introduction and data representation

A first general result of the experiments is that the mechanical MACCEPA model proposed for the actuator in Equation (3) is a good approximation of the actual device. The actual torque provided by the actuator is about 10 percent lower than the target torque which has been used to calculate the trajectory. This can be explained by the limitation of the output motor not being able to provide the peak torques. The angular pattern that is provided by the output motor will be used as input to the simulation to guarantee a valid comparison.

As discussed in Section 1, thanks to the concept of the power amplification in the series elastic element we need a lower power peak in our actuator motor compared to the output motor. Figure 7 shows the power at the input of the motor driver for both the output motor and the actuator motor, averaged over 10 cycles with a precompression of 8mm and a walking duration of 3 seconds/stride in one of the first experiments performed with the setup. The experiment is the same as described before, where the output motor applies the healthy gait ankle angles and the output motor applies the calculated moment arm positions. It is clear that the output motor requires a power peak which is 40% higher than the actuator motor for the same torque output, while the energy input of both motors per stride is almost the same: 122 J/stride for the actuator motor versus 126 J/stride for the output motor).

Figure 8 shows an overview of the averaged test results for one of the experiments. The experiment is performed at a walking duration of 2 seconds per stride and the actuator has a precompression length of 8 mm. This experiment is in the middle of the testing range both in precompression and walking duration and shows the measured power at the different components of the actuation unit. This is an average of several strides, in this case 20. Table 1 shows the energy consumption over one stride at all of the measurement points and

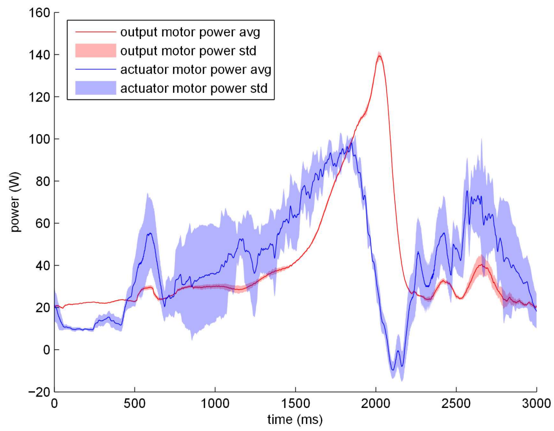

Fig. 7 Comparison between power at the output side of the test setup and at the actuator side in one of the experiments at 3 seconds/stride. The peak power at the output of the setup is 40% higher when compared to the actuator side.

Table 1 Energy and efficiency of the actuator at different components. The energy is calculated by integrating the power over the average of all the strides performed with the same settings, the efficiency is with respect to the source power and the energy loss is with respect to the previous measurement point.

measurement point	energy	efficiency	energy loss
source power	64.5 J	100%	0%
driver power	42 J	65.1%	34.9%
motor power	33 J	51.2%	21.4%
link power	15.4 J	23.9%	53.3%
output power	12 J	18.6%	22.1%

the efficiency of the actuator up to each of the points. The energy consumption is calculated by integrating the power over one stride and the efficiency is calculated compared to the energy at the power source level. The energy loss shows the loss in the components in between the different measurement points and is always referenced to the previous reference point.

4.2 Measured energy losses

4.2.1 Energy losses over the motor driver.

In this section the energy losses over the motor driver throughout the whole set of experiments is discussed. In the analysis of the results, it became clear that the losses in this component are significant as well as strongly dependent on the precompression and the walking duration. Figure 9 shows the energy losses over the motor driver. The losses vary from 28.6% to 49.3% and show a clear relation with both the walking duration and the precompression. There is an optimum around 11 mm

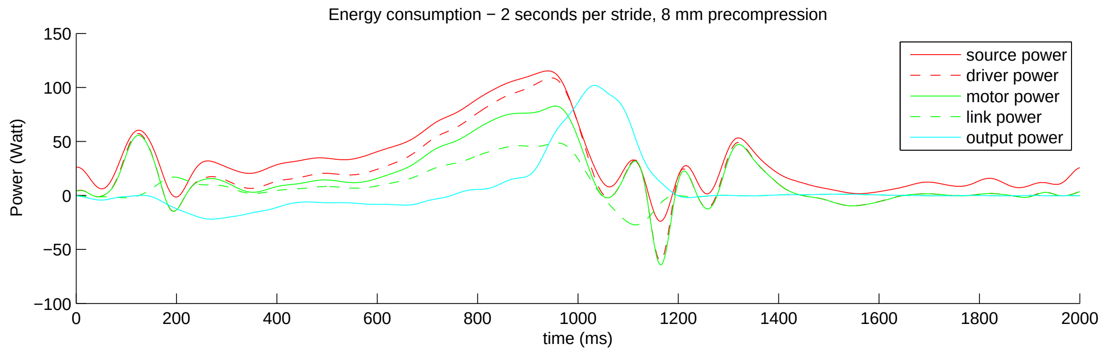

Fig. 8 Overview of the measurement results for the experiment with a precompression of 8 mm performed at 2 seconds per stride. The curves show how the peak power level, the average power level and the peak power position change in the actuator from the power source to the output.

precompression and a walking duration of 1.5 sec/stride and the losses increase for both higher and lower precompressions as well as higher and lower walking velocities. Figure 8 shows that the power loss in the driver (the difference between the source power and the driver power) is spread all over the stride. There is a constant energy consumption in the driver of between 10 and 15 W, which explains why the energy loss per stride is higher at slower walking velocities. The change in efficiency for different precompressions can be explained by the fact that the driver was tuned when the precompression was set to around 8 mm. Changing these parameters for different precompressions may increase the efficiency.

Figure 8 also shows that the negative power that is returned to the driver is not returned to the power source, which further decreases the efficiency of the system. When the driver power has a negative peak to -50 W, the source power only drops to around 0 W.

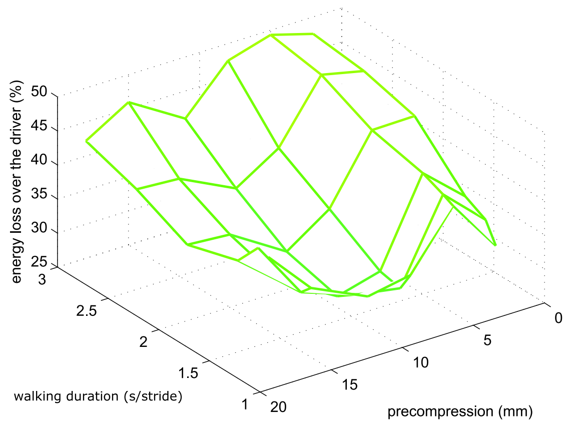

Fig. 9 Energy losses over the motor driver for different walking velocities and spring precompressions.

4.2.2 Motor losses.

The energy losses have been evaluated for the different measurement points at the different precompressions. Figure 10 shows the averaged loss in efficiency for the actuator from the driver to the output for all of the measurements. Two effects can be seen from this graph:

- the motor losses increase with a longer walking duration

- the motor losses increase with a higher precompression

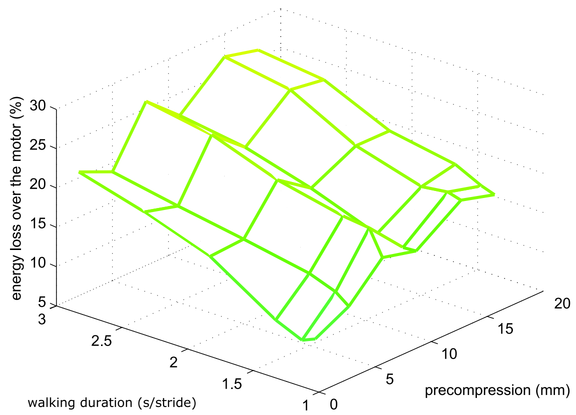

Fig. 10 Energy losses over the motor

Both of these effects can be explained by the fact that the average motor velocity is lower in these cases, resulting in a lower motor efficiency. Figure 8 shows that the losses in the motor mainly occur in the loading phase between 200 and 1000 ms, where the torque increases. This is exactly the phase where the motor has to provide a high torque while the motor velocity is low, which is an ineffective operating mode. At higher precompressions and slower walking velocities, this torque remains more or less the same but the motor velocity decreases so the efficiency is even lower.

4.2.3 Mechanical losses.

Figure 11 shows the energy losses over the gearbox and helical gear used in the actuator while Figure 12 shows the energy losses over the moment arm and the series spring. From the graphs it can be seen that the overall losses in the gearing are very substantial as they are never below 50%. In the case of both high precompression and low walking duration (high walking velocity) however, these losses increase to over 65%. For the output, the average losses are a lot lower, around 20%, yet also at the output the losses increase greatly in the case of both high precompression and low walking duration to over 50% in the worst case. These numbers may seem high but are not surprising as the motor gearbox datasheet already gives a maximum efficiency of the gearbox of 70%. This needs to be multiplied with the efficiency of the helical gear and the efficiencies of the bearings , meaning an overall efficiency of 50% is not unrealistic.

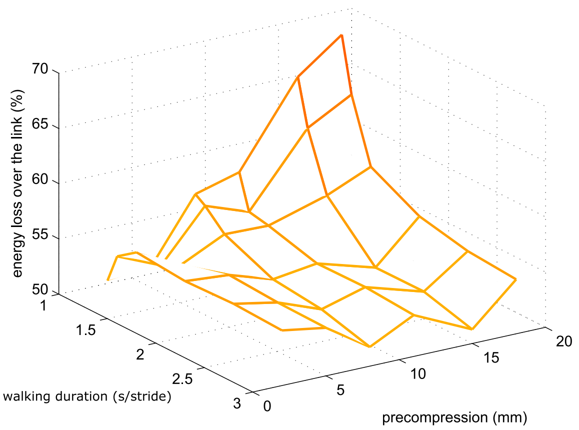

Fig. 11 Energy losses between the output of the motor and the moment arm.

Figure 8 shows that the losses between the motor and the link occur during most of the stride, between 100 and 1500 ms. The link power follows a different curve compared to the motor power, which can be explained by the inertia of the gearbox and the link. Because of this, peaks of motor power for which very clear examples are present around 100 ms and 1300 ms have almost no influence on the link power, causing very large energy losses. Besides this, the losses during the push-off phase (200-1000ms) are very high as the friction losses increase at higher torques.

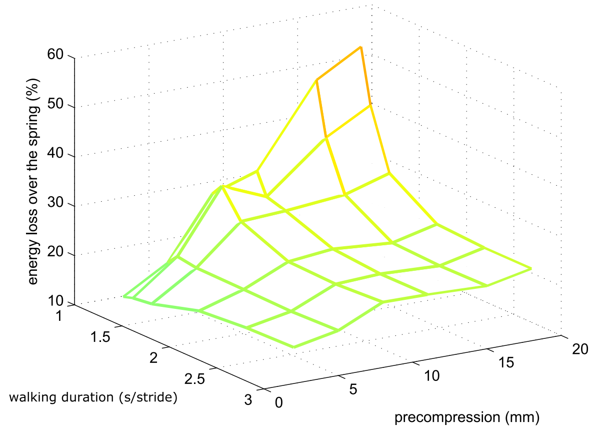

Fig. 12 Energy losses between the moment arm and the output joint.

The peak in mechanical energy losses at high walking velocities is due to reaching the limit of the motor velocity. Figure 13 shows the desired and actual moment arm angle at a precompression of 18 mm and a walking duration of 1.2 s/stride and 3 s/stride. It is clear that the motor cannot follow the setpoint anymore during the push-off phase at the low walking duration. At high precompression values, where the influence of position tracking errors is higher because of the steeper stiffness curve, this leads to a very high mechanical energy loss. This shows that, even though the torque bandwidth of the system is higher for higher precompression values [30], it is better to reduce the precompression at higher walking velocities to be able to track the reference moment arm trajectory.

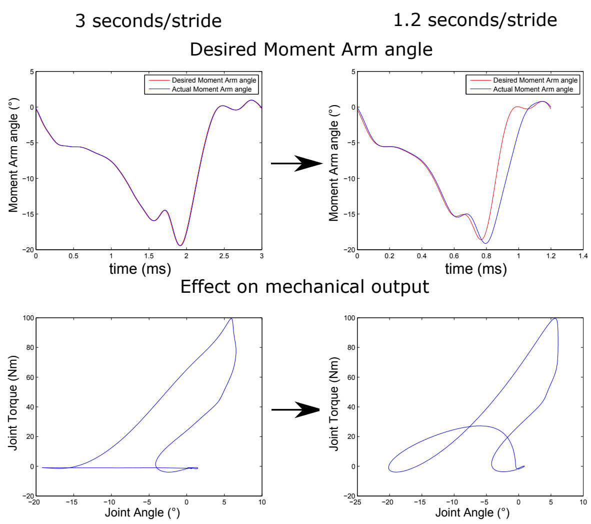

Fig. 13 The upper graphs show the tracking error in the moment arm angle because of a low walking duration. The bottom graphs show the effect of the tracking error on the mechanical output.

4.3 Comparison to modeling results.

The results measured in the test setup are compared to the simulated results using the electromechanical motor model. The first comparison shows that using the original parameters retrieved from the motor datasheet and an estimation of the parameters of the mechanical part don't give a very good approximation when comparing the overall current. Using the torque and angular measurements performed on the device, an optimization of the model was performed, changing the motor parameters to perform a least squares minimization between modeled and measured current over all of the performed measurements at different walking velocities and spring precompressions. Table 4.3 shows the nominal parameters and the resulting parameters of the optimization. The estimated total is the sum of the motor parameters and an estimate of the rest of the actuator. Figure 4.3 shows the difference in behavior of the model before and after optimization compared to the original estimation.

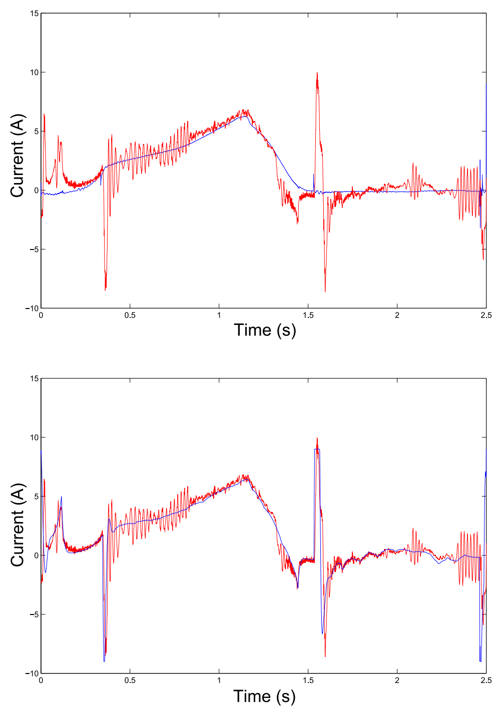

Fig. 14 Comparison between simulated results and measurements before (above) and after (below) optimization of the model parameters.

Figure 15 shows the overall efficiency of the actuator both from the measurements and the simulations. The overall trend is the same in both graphs, but even though the model is optimized there is still a considerable difference between the two graphs. This shows that the model is a good approximation of reality up to a certain level, but there are effects which are not included. There are different possible explanations for this both the mechanical part (error in precompression length, bending of moment arms) and the electrical part of the model (temperature-dependency, driver behavior).

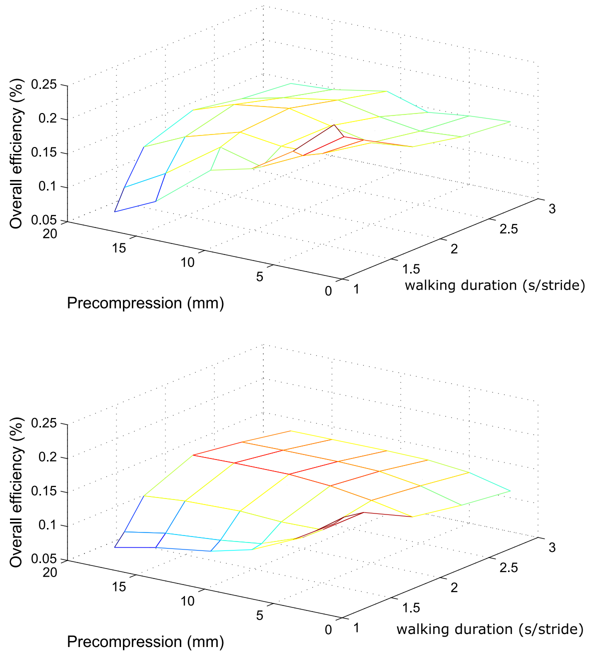

Fig. 15 Overall efficiency of the actuator over a variety of realistic load patterns as measured (a) and simulated with the optimized model (b).

4.4 Optimization of the efficiency

Knowing the model is a good fit for the physical system, we can investigate changes in parameters which are not as easy to change as the precompression and see what the effect is on the energy efficiency.

The actuator was designed based on an optimization of the peak mechanical power at a walking duration of 1.2m/s, taking into account the spring constant and precompression and ending up with a spring stiffness of 130000 N/m and a precompression distance of 7mm [31]. Incorporating the model obtained in this paper we can compare this to the optimum achieved by minimizing the overall electrical power consumption. Figure 16 however shows that this is not in the most energy efficient region of the actuator. The simulation shows that a much higher efficiency can be achieved mainly at lower spring stiffnesses.

The same simulation for a longer simulated walking duration, shown in Figure 17, shows that the average efficiency of the actuator is higher for the same parameter

parameter	unit	motor parameter	estimated total	optimized total
actuator inertia	kgm^2	$5.68E^{-6}$	$1.6E^{-5}$	$3.5E^{-3}$
actuator friction	$Nm * s/rad$	$3.33E^{-6}$	$1.3E^{-4}$	$6E^{-3}$
actuator resistance	Ω	0.386	0.7	2
actuator inductance	H	6.53 E^{-5}	6.53 E^{-5}	6.53 E^{-5}

Table 2 Overview of the motor parameters that have been optimized, with their initial and optimized values.

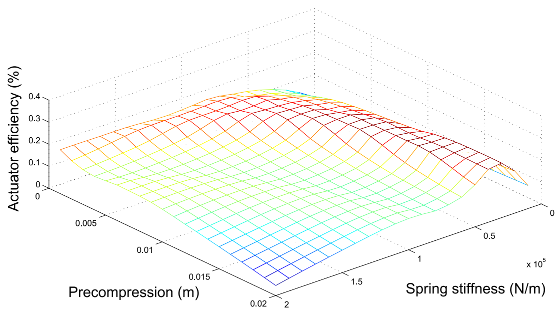

Fig. 16 Optimization of the energy efficiency for a normal walking duration of 1.2 seconds per step. The actuator behavior is simulated for different spring stiffnesses and precompressions.

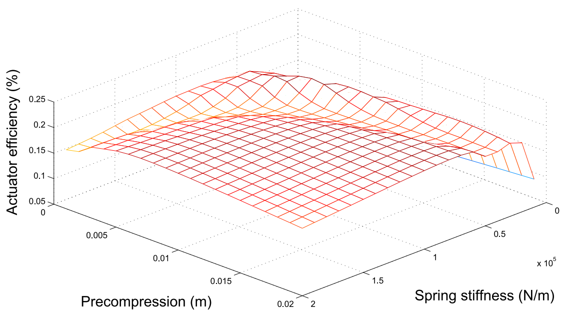

Fig. 17 Optimization of the energy efficiency for a higher walking duration of 2 seconds per step. The actuator behavior is simulated for different spring stiffnesses and precompressions.

range. This graph shows that for these lower walking velocities, it can be worthwhile changing the precompression to a higher value for some spring stiffnesses compared to normal walking. The optimal parameters will depend on the average and also minimum/maximum walking velocity of the amputee.

5 Discussion

The experiments that are performed on the CYBERLEGs Alpha-Prosthesis variable stiffness actuator give an indication on what the efficiency is like during a realistic walking cycle and how it can be optimized. Even though the prosthesis has already been tested with the help of amputee test subjects, the authors believed that the energy measurements during those first experiments were not consistent enough to provide accurate results. As it is expected that there is a learning curve for the amputee and a high amount of training is needed to reach a gait cycle which is both representative and repeatable. For this reason, the test setup discussed in this paper was developed and an average healthy gait cycle was imposed on the actuator. The cycle was very repetitive and constant throughout all of the experiments. In total, the actuator performed over 500 stride cycles at 30 different parameter settings. The measurements from these experiments have been averaged and showed a low deviation. All of the losses and efficiencies seen in the test results could be explained and linked to the actuator parameters.

The energetic consumption of the precompression motor has been neglected in comparison to that of the actuation motor. The assumption is made that this 8W motor is only used when switching from one walking duration to another, to change the precompression to the optimal value. The precompression was altered in between the experiments and the motor didn't consume any energy during the experiments.

The aim of the design of the actuator was to reduce the peak power of the actuator, which is a common practice found in several actuator design and actuator optimization research papers. The test results show that this mechanical power peak is indeed reduced using series elasticity in the actuator, however this does not imply that the actuator is necessarily energy efficient. Even though the electric motors that are used are known for their high energy efficiency, they are used in an operating region where there are high energy losses (low motor velocities, high torques). Also, other parts of the actuator cause high energy losses which were not considered in the initial design of the actuator. There is a considerable energy loss in the motor driver for example, which could be reduced by investigating the possibility of switching of the motor when not providing significant torque, in combination with a non-backdriveable transmission. This of course has an influence on the mechanical energy loss further in the actuator chain, which will increase, but might have an overall positive effect.

The performed measurements could be used to verify the validity of using an electromechanical motor model to optimize the energy consumption of the actuator. Once the model parameters were fitted to the measurements, it could be used to investigate and optimized the energy consumption of the actuator. Whereas in the design of the actuator the amount mechanical energy was used to optimize the parameters, this does not necessarily mean those parameters are optimized for energy efficiency. Indeed, the result of the simulations show that the overall efficiency can be increased by over 10 % by choosing a different set of parameters. The simulations show that the higher efficiencies correspond to a lower spring stiffness which implies a higher motor velocity.

As mentioned before, the efficiencies measured and simulated in this work might come over as low, suggesting bad mechanical implementation or design. The authors believe that this is inherent to the ankle trajectory and the amount of mechanical energy added into the gait cycle at this joint. Active knee joint prosthetic actuators show the same effect: the knee joint is an energy dissipating joint (negative mechanical output energy), active actuators like still consume energy when approximating this trajectory, which means that a similar analysis on those actuators and trajectories would lead to a negative overall efficiency. This shows that this number must be seen in the right perspective and not be compared to, for example motor, efficiencies, which tend to be higher.

The lower spring stiffness in combination with the same motor will lead to a lower actuator bandwidth, which is not taken into account in the analysis. This leads to a less responsive system which is more difficult to stabilize when controlled using closed-loop output position control. However, the actuator in this application is not intended to be used in output closed loop but rather uses the feedback of the moment arm position, which is not influenced by the lower stiffness for the low level control, apart from the fact that the required motor velocity will have to be higher.

6 Conclusion

Optimizing the parameters of an actuator by reducing mechanical output energy and power peak, which has been done for several state-of-the-art actuators and mechanisms, does not necessarily lead to an energy efficient system. The analysis of the energy efficiency of the actuator was performed in this work, showing where energy losses occur and how these could be minimized. Including the electromechanical behavior of an actuator for the optimization, the energy efficiency can be increased from 15% to 25% with respect to optimized parameters only taking mechanical properties into account, which is a considerable difference.

Acknowledgements The first author is funded by a Ph.D. grant from Flanders Innovation & Entrepreneurship (VLAIO). This work has been partially funded by the European Commissions 7th Framework Program as part of the CYBERLEGs project under grant no.287894 and by the and by the Research Foundation-Flanders (FWO) under grant number G.0262.14N.

References

1. Dillingham, T.R., Pezzin, L.E., MacKenzie, E.J.: Limb amputation and limb deficiency: epidemiology and recent trends in the united states. Southern medical journal **95**(8), 875–884 (2002)
2. Ephraim, P.L., Dillingham, T.R., Sector, M., Pezzin, L.E., MacKenzie, E.J.: Epidemiology of limb loss and congenital limb deficiency: a review of the literature. Archives of physical medicine and rehabilitation **84**(5), 747–761 (2003)
3. Herr, H.M., Grabowski, A.M.: Bionic ankle–foot prosthesis normalizes walking gait for persons with leg amputation. Proceedings of the Royal Society B: Biological Sciences **279**(1728), 457–464 (2012)
4. Malcolm, P., Quesada, R.E., Caputo, J.M., Collins, S.H.: The influence of push-off timing in a robotic ankle-foot prosthesis on the energetics and mechanics of walking. Journal of neuroengineering and rehabilitation **12**(1), 1 (2015)
5. Sup, F., Bohara, A., Goldfarb, M.: Design and control of a powered transfemoral prosthesis. The International journal of robotics research **27**(2), 263–273 (2008)
6. Bergelin, B.J., Voglewede, P.A.: Design of an active ankle-foot prosthesis utilizing a four-bar mechanism. Journal of Mechanical Design **134**(6), 061,004 (2012)
7. Everarts, C., Dehez, B., Ronsse, R.: Variable stiffness actuator applied to an active ankle prosthesis: Principle, energy-efficiency, and control. In: 2012 IEEE/RSJ International Conference on Intelligent Robots and Systems, pp. 323–328. IEEE (2012)
8. Au, S.K., Herr, H., Weber, J., Martinez-Villalpando, E.C.: Powered ankle-foot prosthesis for the improvement of amputee ambulation. In: Engineering in Medicine and Biology Society, 2007. EMBS 2007. 29th Annual International Conference of the IEEE, pp. 3020–3026. IEEE (2007)
9. Bellman, R.D., Holgate, M.A., Sugar, T.G.: Sparky 3: Design of an active robotic ankle prosthesis with two actuated degrees of freedom using regenerative kinetics. In: Biomedical Robotics and Biomechatronics, 2008. BioRob 2008. 2nd IEEE RAS & EMBS International Conference on, pp. 511–516. IEEE (2008)
10. Paluska, D., Herr, H.: The effect of series elasticity on actuator power and work output: Implications for robotic and prosthetic joint design. Robotics and Autonomous Systems **54**(8), 667 – 673 (2006). Morphology, Control and Passive Dynamics
11. Zhu, J., Wang, Q., Wang, L.: On the design of a powered transtibial prosthesis with stiffness adaptable ankle and toe joints. Industrial Electronics, IEEE Transactions on **61**(9), 4797–4807 (2014)

12. Vanderborght, B., Van Ham, R., Lefeber, D., Sugar, T.G., Hollander, K.W.: Comparison of mechanical design and energy consumption of adaptable, passive-compliant actuators. The International Journal of Robotics Research **28**(1), 90–103 (2009)
13. Grimmer, M., Seyfarth, A.: Stiffness adjustment of a series elastic actuator in an ankle-foot prosthesis for walking and running: The trade-off between energy and peak power optimization. In: Robotics and Automation (ICRA), 2011 IEEE International Conference on, pp. 1439–1444. IEEE (2011)
14. Hollander, K.W., Sugar, T.G., Herring, D.E.: Adjustable robotic tendon using a'jack spring'. In: Rehabilitation Robotics, 2005. ICORR 2005. 9th International Conference on, pp. 113–118. IEEE (2005)
15. Jafari, A., Tsagarakis, N.G., Sardellitti, I., Caldwell, D.G.: How design can affect the energy required to regulate the stiffness in variable stiffness actuators. In: Robotics and Automation (ICRA), 2012 IEEE International Conference on, pp. 2792–2797. IEEE (2012)
16. Velasco, A., Gasparri, G.M., Garabini, M., Malagia, L., Salaris, P., Bicchi, A.: Soft-actuators in cyclic motion: Analytical optimization of stiffness and pre-load. In: IEEE-RAS International Conference on Humanoid Robots. Atlanta, Georgia, USA (2013)
17. Eslamy, M., Grimmer, M., Seyfarth, A.: Effects of unidirectional parallel springs on required peak power and energy in powered prosthetic ankles: comparison between different active actuation concepts. In: Robotics and Biomimetics (ROBIO), 2012 IEEE International Conference on, pp. 2406–2412. IEEE (2012)
18. Grimmer, M., Eslamy, M., Gliech, S., Seyfarth, A.: A comparison of parallel-and series elastic elements in an actuator for mimicking human ankle joint in walking and running. In: Robotics and Automation (ICRA), 2012 IEEE International Conference on, pp. 2463–2470. IEEE (2012)
19. Realmuto, J., Klute, G., Devasia, S.: Nonlinear passive cam-based springs for powered ankle prostheses. Journal of Medical Devices **9**(1), 011,007 (2015)
20. Verstraten, T., Mathijssen, G., Furnémont, R., Vanderborght, B., Lefeber, D.: Modeling and design of geared dc motors for energy efficiency: Comparison between theory and experiments. Mechatronics **30**, 198–213 (2015)
21. Verstraten, T., Beckerle, P., Furnmont, R., Mathijssen, G., Vanderborght, B., Lefeber, D.: Series and parallel elastic actuation: Impact of natural dynamics on power and energy consumption. Mechanism and Machine Theory. (2016)
22. Au, S.K., Herr, H.: Powered ankle-foot prosthesis. Robotics & automation magazine, IEEE **15**(3), 52–59 (2008)
23. Holgate, M.A., Hitt, J.K., Bellman, R.D., Sugar, T.G., Hollander, K.W.: The sparky (spring ankle with regenerative kinetics) project: Choosing a dc motor based actuation method. In: Biomedical Robotics and Biomechatronics, 2008. BioRob 2008. 2nd IEEE RAS & EMBS International Conference on, pp. 163–168. IEEE (2008)
24. Rouse, E.J., Mooney, L.M., Martinez-Villalpando, E.C., Herr, H.M.: Clutchable series-elastic actuator: Design of a robotic knee prosthesis for minimum energy consumption. In: Rehabilitation Robotics (ICORR), 2013 IEEE International Conference on, pp. 1–6. IEEE (2013)
25. Beckerle, P., Wojtusch, J., Schuy, J., Strah, B., Rinderknecht, S., Stryk, O.: Power-optimized stiffness and nonlinear position control of an actuator with variable torsion stiffness. In: Advanced Intelligent Mechatronics (AIM), 2013 IEEE/ASME International Conference on, pp. 387–392. IEEE (2013)
26. Ambrozic, L., Gorsic, M., Geeroms, J., Flynn, L., Molino Lova, R., Kamnik, R., Munih, M., Vitiello, N.: Cyberlegs: A user-oriented robotic transfemoral prosthesis with whole-body awareness control. Robotics & Automation Magazine, IEEE **21**(4), 82–93 (2014)
27. Giovacchini, F., Vannetti, F., Fantozzi, M., Cempini, M., Cortese, M., Parri, A., Yan, T., Lefeber, D., Vitiello, N.: A light-weight active orthosis for hip movement assistance. Robotics and Autonomous Systems **73**, 123–134 (2015)
28. Tropea, P., Vitiello, N., Martelli, D., Aprigliano, F., Micera, S., Monaco, V.: Detecting slipping-like perturbations by using adaptive oscillators. Annals of biomedical engineering pp. 1–11 (2014)
29. Van Ham, R., Vanderborght, B., van Damme, M., Verrelst, B., Lefeber, D.: MACCEPA, the mechanically adjustable compliance and controllable equilibrium position actuator: Design and implementation in a biped robot. Robotics and Autonomous Systems **55 (10)**, 761–768 (2007)
30. Jimenez-Fabian, R., Flynn, L., Geeroms, J., Vitiello, N., Vanderborght, B., Lefeber, D.: Sliding-bar maccepa for a powered ankle prosthesis. Journal of Mechanisms and Robotics **7**(4), 041,011 (2015)
31. Flynn, L., Geeroms, J., Jimenez-Fabian, R., Vanderborght, B., Vitiello, N., Lefeber, D.: Ankle–knee prosthesis with active ankle and energy transfer: Development of the cyberlegs alpha-prosthesis. Robotics and Autonomous Systems **73**, 4–15 (2015)
32. Winter, D.A.: Biomechanics and Motor Control of Human Movement. John Wiley and Sons, United States of America (2005)